Inorganic Chemistry
Article
Cite This: Inorg. Chem. 2019, 58, 14058−14067
pubs.acs.org/IC

Expanding the Doubly Cation Ordered $AA'BB'O_6$ Perovskite Family: Structural Complexity in $NaLaInNbO_6$ and $NaLaInTaO_6$

Graham King*,† and Susana Garcia-Martin‡

†Canadian Light Source, Inc., 44 Innovation Boulevard, Saskatoon, Saskatchewan S7N 2V3, Canada
‡Departamento de Química Inorgánica I, Facultad de Ciencias Químicas, Universidad Complutense, 28040 Madrid, Spain

Supporting Information

ABSTRACT: Two new perovskite compounds, $NaLaInNbO_6$ and $NaLaInTaO_6$, have been synthesized. Both compounds have a rock-salt ordering of the In/Nb or In/Ta cations and a layered ordering of the Na/La. They are unusual among this family of doubly cation ordered perovskites for having a +3/+5 combination of B/B' oxidation states instead of a divalent cation and W^{6+}. Synchrotron powder diffraction and electron diffraction data show both compounds have tetragonal $\sqrt{2}a_p \times \sqrt{2}a_p \times 2a_p$ unit cells. The octahedral tilt system of these compounds is complicated and seems to vary depending on the length scale considered. Bond valence considerations demonstrate that none of the tilt systems compatible with a tetragonal unit cell produce a stable structure. It is proposed that additional oxygen displacements are occurring on a local scale. The XRD data show that the B-site ordering is nearly complete in both cases, while the A-site cations show a lower degree of order. The tendency of the B'-cation to undergo a second order Jahn−Teller distortion is identified as having an influence over the degree of A-site ordering. Transmission electron microscopy shows fragmentation into nanosized domains with perpendicular orientations of the layered A-site cation ordering. Such structures may be polar over short length scales which could lead to interesting dielectric properties such as relaxor behavior. The prospects for finding new doubly cation ordered perovskites are also discussed.

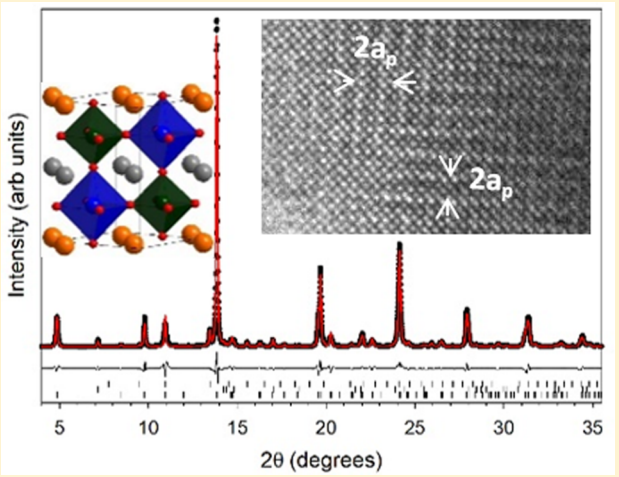

1. INTRODUCTION

The perovskite structure is among the most heavily studied in all of solid state chemistry. While simple ABX_3 perovskites possess structural variety due to distortions such as octahedral tilting and Jahn−Teller displacements,[1−3] the more complex structures of cation ordered perovskites lead to many of the most fascinating and desirable properties. The lower symmetry and interactions between cations can lead to new behavior not possible in simpler compositions. While there is a wide variety of possible cation ordering patterns, only a few are commonly observed.[4] The most common type of cation ordering is a rock-salt ordering of two B-site cations to give the $A_2BB'X_6$ double perovskite structure.[5] Ordering of A-site cations is less common but can occur under certain conditions. A 3:1 pattern is stabilized in $AA'_3B_4O_{12}$ compositions by a particular pattern of octahedral tilting and Jahn−Teller distortions of smaller cations residing on the A'-sites.[6] A layered pattern of A-site ordering is more common and is usually stabilized by the presence of anion vacancies for $RBaB_2O_{5+\delta}$ compositions,[7,8] or by A-site vacancies in combination with second order Jahn−Teller (SOJT) displacements of highly charged d^0 B-site cations such as in $La_{2/3-x}Li_xTiO_3$ compositions.[9]

While ordering on either the A- or B-sites lowers the symmetry and opens up new possibilities for materials design, simultaneous ordering on both cation sublattices can lead to even more complex structures and unlock properties that are not possible in perovskites with ordering on only a single cation sublattice. The doubly ordered $AA'BB'O_6$ structure type combines both rock-salt ordering of B/B' and layered ordering of A/A' without vacancies (Figure 1). There were few examples of this structure type until a little over a decade ago when the structural stabilizing forces were first recognized, allowing a targeted search for new members.[10−14] The layered A-site ordering is stabilized by the presence of a SOJT distortion of one of the B-site cations.[14] It also appears linked to the B-site ordering as only short-range A-site order is observed in compositions with a single B-site cation or with a disordered arrangement of two B-site cations, even if a SOJT cation is present.[14,15] This family of compounds has some of the most complex structures known among perovskites, including features which are attractive for engineering new materials. Most of the structures can be broken down into two

Received: July 9, 2019
Published: October 9, 2019

DOI: 10.1021/acs.inorgchem.9b02050
Inorg. Chem. 2019, 58, 14058−14067

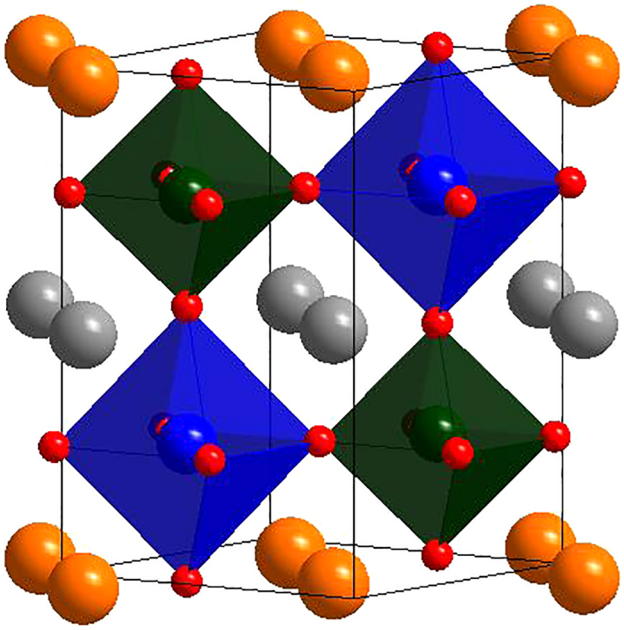

Figure 1. Doubly cation ordered $AA'BB'O_6$ perovskite structure type. A are large gray, A' are large orange, B are blue, B' are dark green, and O are small red spheres. This figure shows the aristotype structure without any octahedral tilting.

classes, those with $a^-a^-c^+$ octahedral tilting and those which form large superstructures based on $a^-a^-c^0$ tilting.

The characteristic that has perhaps caught the most attention is the polar nature of many members of this family. The ordering of both cation sublattices along with the most common pattern of octahedral tilting known for perovskites ($a^-a^-c^+$ in Glazer notation) leads to the noncentrosymmetric space group $P2_1$.[14] The inversion symmetry is not broken by the SOJT displacements, as happens in other perovskite systems, as these are aligned antiferroelectric in these compounds. Rather, the polarization stems from nonequivalent displacements of the differently charged A and A' cations.[16] The possibility to have magnetic cations on either the A or B sublattices also makes them interesting magnetic materials.[17−19] Particularly complex magnetic structures have been found when magnetic cations are present on both sublattices due to interactions between the two.[20] The existence of magnetism within a polar structure has generated interest in this class of materials as potential multiferroics.[21−23] The first experimental attempts to measure ferroelectricity in these materials did not find any, which is puzzling considering the structural results.[24] It has recently been suggested by theoretical and new experimental studies that these materials have large barriers to switching and may be best described as having nonswitchable polarizations.[16,25] The lack of inversion symmetry is also beneficial for optical properties. A number of recent studies have used $AA'BB'O_6$ perovskites as host materials for doping with other lanthanides to create phosphors.[26−35] The results have been quite promising and have been attributed to the lower symmetry at the A-sites being beneficial to the ligand field around the phosphor ions.

Other $AA'BB'O_6$ perovskite compounds have been found to form large but very subtle superstructures. At least part of the origin of these superstructures comes from a twinning of the octahedral tilt system. These compounds have been proposed to have an $a^-a^-c^0$ tilt pattern where the out-of-phase tilting is periodically interrupted by an in-phase tilt in either one or both directions.[36] Another model has been proposed in which the amplitude of the tilting about the c-axis varies from being pronounced to being nearly absent near the twin boundaries.[37] This model attributes the formation of the superstructures to a competition between the SOJT distortions and the octahedral tilting. In either case it seems apparent that a twinning of the out-of-phase components of the tilt system is present. Some studies have suggested that a variation in the A-site occupancies occurs with the same periodicity for certain compositions.[38,39] The most recent studies suggest that the composition is different at the twin boundaries, although the nature of these compositional modulations is still not well-understood and is a matter of ongoing debate.[40,41] A wide variety of superstructure sizes and dimensions have been observed. $NaLaMgWO_6$ and $NaLaCoWO_6$ have been found to have one-dimensional stripe patterns with periodicities of $12a_p$, where a_p is the length of the basic perovskite subcell (∼3.9 Å).[36,38,42] $KLaMnWO_6$ and $NaNdMgWO_6$ have two-dimensional checkerboard patterns with periodicities of $10a_p$ and $14a_p$, respectively.[39,43] $NaCeMnWO_6$, $NaPrMnWO_6$, and $KLaCaWO_6$ are found to have incommensurately modulated structures.[44,45] $NaLaCaWO_6$, $NaPrCoWO_6$, and $NaNdCoWO_6$ have a different stripe pattern which goes along the ⟨110⟩ direction instead of the ⟨100⟩ direction and has a periodicity of $16a_p$ in all three cases.[40,42]

An important lesson that has emerged from these studies is that standard X-ray powder diffraction (XRD) cannot reliably determine the structure of a doubly ordered $AA'BB'O_6$ perovskite. The superstructures that sometimes form as a result of subtle variations in the tilting of the light oxygen octahedra are undetectable by laboratory based XRD and sometimes even by synchrotron XRD.[36] In order to conclusively characterize such structures, electron diffraction and/or neutron diffraction is required. However, from the known examples some trends have emerged. Those compounds which appear to have a $P2_1$ structure according to XRD have always been confirmed to have this space group when examined by neutron diffraction.[17,22,28,45] Those that appear to have $P4/nmm$ symmetry are found to have superstructures formed by twinning in two dimensions.[39,43] Those which appear to have space group $C2/m$ are found to have twinning along one direction.[36,38,42,45] The limited ability of XRD to study this structure type is not always recognized, particularly in the case of phosphor research. There have been numerous recent studies which have claimed $C2/m$ structures based purely on laboratory XRD data. These conclusions are most likely incorrect as this space group and its corresponding $a^0b^-c^0$ tilt system have never been observed when such materials are probed by more sensitive techniques. Reports of $C2/m$ structures even persist for compounds whose host compositions have already been conclusively shown not to be $C2/m$, such as $NaLaMgWO_6$. Those working in the phosphor field who use only XRD data are encouraged to mention the limitations of this method and the possibility of an undetected superstructure. Table 1 lists all of the known $AA'BB'O_6$ perovskites and can be used as a reference to see what is known about a host composition's structure.

The family of doubly ordered perovskites has grown considerably over recent years and is now of moderate size with more than 45 members. Table 1 lists, to the best of our knowledge, all of the known $AA'BB'O_6$ perovskite compounds. One feature that stands out is that nearly all of these

DOI: 10.1021/acs.inorgchem.9b02050
Inorg. Chem. 2019, 58, 14058−14067

Table 1. List of All Known Doubly Cation Ordered $AA'BB'O_6$ Perovskites[a]

composition	characterization	structure	τ	ref
$KLaMgWO_6$	XRD, NPD	SS	1.01	31, 46
$LiLaMgWO_6$	XRD	$P4/nmm$ (?)	0.893	29, 46
$NaLaMgWO_6$	XRD, NPD, TEM	SS 12 × 2 × 2	0.952	10, 14, 36, 38
$NaCeMgWO_6$	XRD	$P4/nmm$ (?)	0.948	18
$NaPrMgWO_6$	XRD	$P4/nmm$ (?)	0.946	18
$NaNdMgWO_6$	SXRD, NPD, TEM	SS 14 × 14 × 2	0.940	17, 18, 43
$NaSmMgWO_6$	XRD	$P2_1$ (?)	0.937	18
$NaEuMgWO_6$	XRD	$P2_1$ (?)	0.935	18
$NaGdMgWO_6$	SXRD	$P2_1$	0.933	18, 28
$NaTbMgWO_6$	XRD	$P2_1$ (?)	0.927	18
$NaDyMgWO_6$	XRD	$P2_1$ (?)	0.922	18
$NaHoMgWO_6$	XRD	$P2_1$ (?)	0.926	18
$NaYMgWO_6$	SXRD, NPD	$P2_1$	0.922	28
$KLaMnWO_6$	SXRD, NPD, TEM	SS 10 × 10 × 2	0.986	17, 39
$NaLaMnWO_6$	XRD, NPD	$P2_1$	0.930	17, 20
$NaCeMnWO_6$	SXRD, NPD, TEM	SS IC	0.926	18, 44
$NaPrMnWO_6$	SXRD, NPD, TEM	SS IC	0.924	18, 44
$NaNdMnWO_6$	XRD, NPD	$P2_1$	0.918	17, 20
$NaSmMnWO_6$	XRD	$P2_1$ (?)	0.915	18
$NaGdMnWO_6$	XRD	$P2_1$ (?)	0.911	18
$NaTbMnWO_6$	XRD, NPD	$P2_1$	0.906	17, 20
$NaDyMnWO_6$	XRD	$P2_1$ (?)	0.900	18
$NaHoMnWO_6$	XRD	$P2_1$ (?)	0.904	18
$NaYMnWO_6$	XRD	$P2_1$ (?)	0.900	25
$NaLaNiWO_6$	XRD	$P2_1/m$ (?)	0.956	13
$NaLaCoWO_6$	SXRD, TEM, SHG	SS 12 × 2 × 2	0.952	13, 45
$NaPrCoWO_6$	SXRD, TEM,, SHG	SS 16 (110)	0.946	45
$NaNdCoWO_6$	SXRD, NPD, TEM, SHG	SS 16 (110)	0.940	17, 45
$NaSmCoWO_6$	SXRD, SHG	$P2_1$	0.937	45
$NaEuCoWO_6$	SXRD, SHG	$P2_1$	0.935	45
$NaGdCoWO_6$	SXRD, SHG	$P2_1$	0.933	45
$NaTbCoWO_6$	SXRD, NPD, SHG	$P2_1$	0.928	45
$NaDyCoWO_6$	SXRD, SHG	$P2_1$	0.922	45
$NaHoCoWO_6$	SXRD, NPD, SHG	$P2_1$	0.926	25, 45
$NaYCoWO_6$	SXRD, NPD, SHG	$P2_1$	0.922	45
$NaErCoWO_6$	SXRD, SHG	$P2_1$	0.920	45
$NaYbCoWO_6$	SXRD, SHG	$P2_1$	0.916	45
$NaLaFeWO_6$	XRD, NPD, TEM, SHG	$P2_1$	0.942	22
$NaPrFeWO_6$	XRD, NPD	$P2_1$	0.936	23
$NaNdFeWO_6$	XRD, NPD, TEM, SHG	$P2_1$	0.931	22
$NaSmFeWO_6$	XRD, NPD	$P2_1$	0.928	23
$KLaCaWO_6$	XRD, TEM	SS IC	0.945	40
$NaLaCaWO_6$	XRD, TEM	SS 16 (110)	0.891	40
$KYCaWO_6$	XRD	$C2/m$ (?)	0.917	33
$KLuCaWO_6$	XRD	$C2/m$ (?)	0.912	33
$NaLaScNbO_6$	XRD, NPD	SS	0.936	14, 46

[a]Doped compositions are not included, only the parent compositions. The characterization column lists the methods which have been used for structural analysis (XRD = laboratory powder X-ray diffraction, SXRD = synchrotron powder diffraction, NPD = neutron powder diffraction, TEM = transmission electron microscopy, SHG = second harmonic generation). In the structure column the space group is listed if no superstructure is present; a question mark indicates that the structural characterization is preliminary and cannot rule out the possibility of a superstructure. An SS in this column indicates there is a superstructure; the dimensions of the superstructure are listed in unit of a_p if determined (IC means incommensurately modulated). The tolerance factors (τ) have been calculated using SPuDS.[5].

compounds have +2/+6 oxidation states for the B/B' cations with W^{6+} serving as the SOJT cation. In this work we were interested in going in a new direction by searching for members which fall outside of the dominant +2/+6 pattern. There is just a single report of a compound with a +3/+5 cation combination where Nb^{5+} acts as the SOJT cation, $NaLaScNbO_6$.[14,46] The related compound $NaLaMg_{2/3}Nb_{4/3}O_6$ is also known.[47] Obtaining +3/+5 compounds can be more challenging, as the smaller charge difference makes stabilizing B-site ordering, and therefore A-site ordering, more difficult. Such compounds might be unstable relative to forming $A^{+1}B^{+5}O_3$ and $A^{+3}B^{+3}O_3$ single perovskite phases, an issue not present with +2/+6 combinations. Using a +3/+5 cation combination also opens up new possibilities, such as having partial cation ordering on both sublattices. As the +3/+5 compounds are almost completely unexplored, we wanted to

DOI: 10.1021/acs.inorgchem.9b02050
Inorg. Chem. 2019, 58, 14058−14067

see if more could be made and how their structures compare to those of the +2/+6 compounds. We have chosen to use In^{3+} as its large size should help promote cation ordering and to use Nb^{5+} and Ta^{5+} as the SOJT cations.[48−50] In this work we report the preparation of two new $AA'BB'O_6$ compounds and their detailed structural analysis using synchrotron XRD, electron diffraction, and transmission electron microscopy.

2. EXPERIMENTAL SECTION

The samples were prepared by the ceramic method. The starting materials used were Na_2CO_3, La_2O_3, In_2O_3, Nb_2O_5, and Ta_2O_5. Stoichiometric amounts of the reagents were ground together with a mortar and pestle. A 25% excess of Na_2CO_3 was used. The powders were pressed into pellets and heated to 1100 °C for 18 h. The samples were then reground with an additional 20% excess of Na_2CO_3, pressed into pellets again, and then reheated to 1150 °C for 12 h. The heating and cooling rates were always around 100 °C per hour. The phase purity was monitored using a laboratory powder X-ray diffractometer.

Synchrotron powder X-ray diffraction data were collected on the CMCF-BM beamline at the Canadian Light Source using an area detector and λ = 0.68422 Å radiation. The $NaLaInNbO_6$ sample was loaded into a capillary with a 0.63 mm inner diameter while a 0.3 mm capillary was used for $NaLaInTaO_6$ due to its greater absorption. The capillaries were spun during data collection. The data were integrated and refined using GSAS-II.[51]

High resolution transmission electron microscopy (HRTEM) and selected area electron diffraction (SAED) were performed with a JEOL JEM 3000F microscope operating at 300 kV (double tilt ±20°), fitted with an X-ray energy dispersive spectroscopy (XEDS) microanalysis system (OXFORD INCA).

3. RESULTS AND DISCUSSION

3.1. Synthesis. The synthesis of these compounds requires a higher temperature than is needed for many other $AA'BB'O_6$ perovskites. Synthetic attempts at temperatures of 1000 °C or below resulted in large amounts of starting materials remaining. The required higher temperatures introduced issues with Na volatility. The challenge in synthesizing these materials was thus finding the right balance between achieving reactivity while not losing too much Na. The synthesis was accomplished by finding the right temperature window along with using a large excess of Na. It was found that long heating times at temperatures between 1100 and 1200 °C were sufficient to induce a reaction while only causing small amounts of Na volatility that could be countered by using an excess. If the temperature was raised above 1200 °C, then major Na loss always occurred and large secondary phases of $LaNbO_4$, La_3NbO_7 (or $LaTaO_4$, La_3TaO_7), and In_2O_3 would form. A slow cooling rate was employed in order to promote the ordering of the cations. Small amounts of In_2O_3 and sometimes $NaInO_2$ were always present and did not diminish with further heating, suggesting that the true compositions of these compounds may not be a 1:1:1:1 ratio of cations but they could be slightly rich in Na and Nb/Ta. This may be another reason why the synthesis always worked better with an excess of Na. A similar deviation from ideal stoichiometry was reported for Ca_2InNbO_6.[48]

3.2. Synchrotron Powder Diffraction. The powder diffraction patterns clearly indicate that both compounds adopt perovskite related structures (Figure 2). In addition to the fundamental perovskite reflections, supercell reflections indicative of both *A*- and *B*-site cation ordering are observed. The *B*-site order is most clearly revealed by the appearance of a $(^1/_2\ ^1/_2\ ^1/_2)$ reflection, as indexed on the undistorted cubic

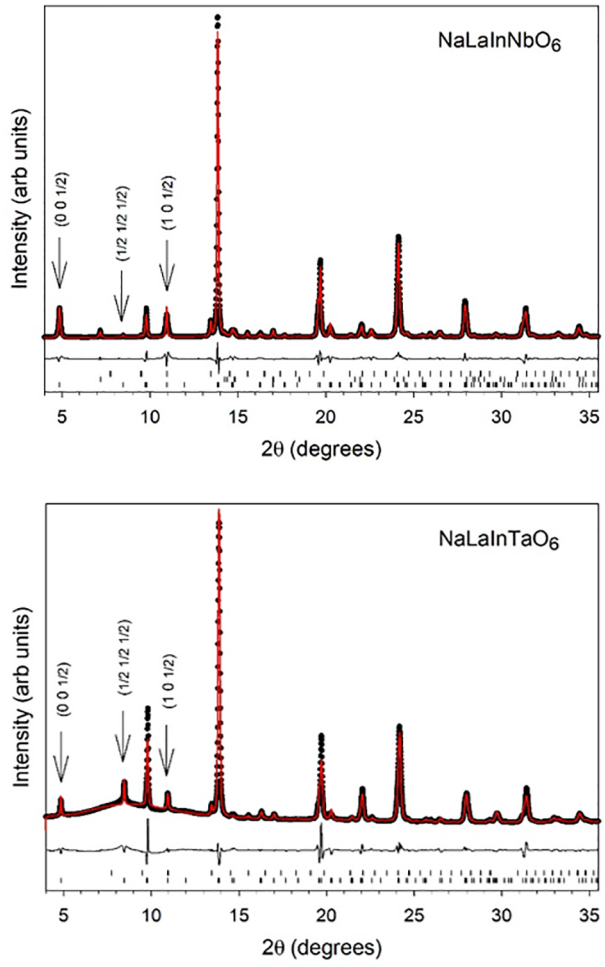

Figure 2. Synchrotron X-ray diffraction patterns (black circles), Rietveld fits (red lines), and difference curves (beneath). The first three cation ordering peaks are labeled as indexed on a cubic a_p unit cell. The upper tick marks are the *hkl* positions for In_2O_3, the bottom tick marks are for the main perovskite phase, and the middle tick marks in the $NaLaInNbO_6$ pattern are for $NaInO_2$.

$Pm\bar{3}m$ a_p perovskite cell. This ordering peak is clearly visible for $NaLaInTaO_6$, but for $NaLaInNbO_6$ it is very weak due to the similar scattering power of In and Nb. The peak can only be clearly observed above the background in the synchrotron data and is not discernible in data collected on a laboratory diffractometer. The *A*-site ordering is revealed by $(0\ 0\ ^1/_2)$ and $(1\ 0\ ^1/_2)$ reflections, which are both clearly seen in both diffraction patterns. It should be noted that the $(1\ 0\ ^1/_2)$ peak for $NaLaInNbO_6$ is distinctly broadened compared to the other peaks in this diffraction pattern. A few weak peaks in each diffraction pattern are attributed to In_2O_3, and the $NaLaInNbO_6$ pattern seems to indicate a small amount of $NaInO_2$ as well.

Both diffraction patterns can be indexed using a $\sqrt{2}a_p \times \sqrt{2}a_p \times 2a_p$ tetragonal unit cell. According to a prior group theoretical analysis, there are 5 tetragonal space groups that can result from double cation ordering and simple octahedral tilt patterns.[14] The aristotype space group corresponding to no octahedral tilting is $P4/nmm$. $P\bar{4}2m$ and $P\bar{4}$ symmetries result from $a^+a^+c^0$ and $a^+a^+c^-$ tilting, respectively. The $a^+a^+c^0$ tilt system has never been observed, and the $a^+a^+c^-$ tilt system is only found to occur with a rare type of columnar *A*-site ordering. Furthermore, these two space group correspond to

DOI: 10.1021/acs.inorgchem.9b02050
Inorg. Chem. 2019, 58, 14058−14067

$2a_p \times 2a_p \times 2a_p$ unit cells, which would allow for peak splitting which is not observed. Therefore, these two possibilities can be safely ruled out. The other two possibilities correspond to in-phase or out-of-phase tilting about the *c*-axis and have $\sqrt{2}a_p \times \sqrt{2}a_p \times 2a_p$ unit cells. $P42_12$ results from $a^0a^0c^+$ tilting. The reflection conditions for this space group are very similar to that of *P*4/*nmm* with the first additional peak occurring at a *d*-spacing of ~2.54 Å. By an unfortunate coincidence the In_2O_3 secondary phase also has a peak at almost the same position, so it cannot be conclusively determined by the XRD data alone if a very weak peak from in-phase tilting is present. While neutron diffraction is often used to resolve tilt systems in perovskites, the strong absorption cross section of In makes collecting high quality data difficult, and the same issue of overlap with the In_2O_3 peak would exist unless high purity samples could be obtained. The *P*4/*n* space group, corresponding to $a^0a^0c^-$ tilting, has the same reflection conditions as *P*4/*nmm* and can only be differentiated by fitting the peak intensities. Another possibility is that a superstructure is present. There are previous examples where a twinning of $a^-a^-c^0$ tilting results in a tetragonal unit cell but with very weak satellite peaks around some primary reflections.[44] However, no satellite peaks are clearly observed in either of these diffraction patterns.

Rietveld refinements were performed using *P*4/*nmm*, $P42_12$, and *P*4/*n* models. All three space groups were able to give a reasonable fit to the diffraction data. The $P42_12$, and *P*4/*n* models each have just a single extra degree of freedom for 2/3 of the O atoms compared to *P*4/*nmm*, so the similarity in fitting is not surprising. For the *P*4/*n* model the O atoms did not move significantly off the high symmetry position they would have in the *P*4/*nmm* model. As the refinement did not make use of this extra degree of freedom, this model does not seem appropriate. The $P42_12$ refinement did produce a distinct tilting of the octahedra, although the quality of the fit was essentially the same as for the *P*4/*nmm* fit. The HRTEM/SAED data, presented in the next section, reveals that the crystals are formed by domains of perpendicular *A*-site ordering and gives indications of an additional reflection relating to out-of-phase tilting. However, the resolution of the data that can be extracted from small domains does not allow for a conclusive space group assignment. It seems that the structures likely have *P*4/*nmm* symmetry when viewed over long length scales but might be best considered as $P42_12$ within the domains-scale. The $a^0a^0c^+$ tilting, which is perpendicular to the layered *A*-site ordering in $P42_12$, would become fragmented along with the *A*-site ordering. The fits using any space group have some minor issues with modeling the peak shapes and intensities, particularly in the case of $NaLaInTaO_6$. This is an indication that the unit cell descriptions of these materials are an average approximation of a more complicated local situation. Lattice parameters are listed in Table 2. The impurity phase fractions by mass refined to 2.97(6)% In_2O_3 and 2.64(6)% $NaInO_2$ in the $NaLaInNbO_6$ sample and 3.4(2)% In_2O_3 in the $NaLaInTaO_6$ sample.

The observation of a tetragonal unit cell is surprising considering that the small tolerance factors of these compositions (0.924 for Nb and 0.922 for Ta) should require octahedral tilting along two or three axes. The atomic coordinates obtained from the Rietveld refinements as well as the bond valence sums are reported in the Supporting Information. It is clear that a stable bonding arrangement cannot be achieved in structures with either *P*4/*nmm* or $P42_12$ symmetry. It would seem that some additional short-range octahedral tilting must be occurring to stabilize the structures. This would be consistent with the fact that the oxygen atomic displacement parameters always refined to large values. It could be that high defect concentrations cause a nonperiodic twinning of the out-of-phase tilting components, making them appear absent in the average structure. A similar nonperiodic twinning has been reported before for another perovskite.[52] The related cation disordered compound $Na_{0.5}Bi_{0.5}Sc_{0.5}Nb_{0.5}O_3$, which has a similar tolerance factor as these compounds, was recently reported to have an average structure with $a^0a^0c^+$ tilting and a large amount of local oxygen disorder.[53] It seems that, apart from differences in cation order, these two compounds may be structurally similar.

Table 2. Information Relating to the Powder Diffraction Data and Refinements

	$NaLaInNbO_6$	$NaLaInTaO_6$
source	synchrotron bending magnet	synchrotron bending magnet
FW (g/mol)	465.61	553.66
temp	ambient	ambient
wavelength (Å)	0.68422	0.68422
cryst syst	tetragonal	tetragonal
space group	*P*4/*nmm* or $P42_12$	*P*4/*nmm* or $P42_12$
a (Å)	5.6663(4)	5.6629(2)
c (Å)	8.0633(4)	8.0589(3)
V (Å^3)	258.88(4)	258.44(3)
Z	2	2
d-space range (Å)	9.8−1.107	9.8−1.107
χ^2	128	24.7
R_p (%)	9.21	4.55
R_{wp} (%)	12.6	6.91

The degree of cation ordering was determined by allowing site mixing between the Na/La over the two *A*-sites and the In/(Nb or Ta) over the two *B*-sites while maintaining overall site occupancies of 1. The results can be given as the long-range order (LRO) parameter, defined as $(2 \times S) - 1$ where *S* is the occupancy of the cation predominantly occupying the site. For example, in $NaLaInTaO_6$ the *B*-site has an occupancy of 95% In and 5% Ta while the *B*′-site has an occupancy of 5% In and 95% Ta, giving a *B*-site LRO of 90%. $NaLaInNbO_6$ is found to also have a *B*-site LRO parameter around 90%, although with a fairly large uncertainty due to the weakness of the ordering peak. Regardless of its exact value, it is still clear that both of these compounds have high levels of *B*-site ordering. The *B*-site ordering may actually be essentially complete within the limits of its composition, with much of the apparent disorder actually coming from the fact that the In:(Nb/Ta) ratio is slightly smaller than 1. In contrast, the Na/La in both compounds show lower levels of ordering. For $NaLaInNbO_6$ the *A*-site LRO parameter is 72% while it is only 50% for $NaLaInTaO_6$. The disorder can arise from having partial ordering within the particles, having a sample consisting of ordered and disordered particles, or having domain formation within particles. The broadness of some of the *A*-site ordering peaks in the XRD data and the HRTEM images reveals that structural-domain formation is definitely occurring and is responsible for at least some of the observed disorder. Considering the degree of disorder, it seems likely that nonstoichiometry and partial ordering within domains may also be contributing. The high concentration of domain

DOI: 10.1021/acs.inorgchem.9b02050
Inorg. Chem. 2019, 58, 14058−14067

boundaries will also lead to a significant portion of the sample having a different structure at the boundary.

Now that compounds with a SOJT cation other than W^{6+} have been obtained, the parameters that control the degree of *A*-site ordering can be better assessed. The W^{6+} compounds all show complete *B*-site ordering and complete or near complete *A*-site ordering. $NaLaInNbO_6$ and $NaLaInTaO_6$ show less *A*-site ordering than the W^{6+} compounds despite having nearly as much *B*-site order, with the Ta compound being less ordered than the Nb compound. This shows a trend of *A*-site LRO decreasing as the *B*′-cation propensity to undergo a SOJT decreases. The relative tendencies of the SOJT cations known for this structure type to displace are in the order $W^{6+} > Nb^{5+} > Ta^{5+}$.[54] Previously, $NaLaScNbO_6$ was reported to have a *B*-site LRO of 84% and an *A*-site LRO of 62%. The lower *A*-site LRO of this compound compared to $NaLaInNbO_6$ can be attributed to the lower degree of *B*-site order. $NaLaScNbO_6$ still shows more *A*-site order than $NaLaInTaO_6$ despite having less *B*-site order, showing that the SOJT nature of the *B*′-cation is indeed important. These comparisons suggest that both factors play a roughly equal role. The ability to control the *A*-site order by the SOJT strength of the *B*′-cation is important as it allows the two order parameters to be tuned somewhat independently. It is also important to keep in mind that for a charge difference of 2 the degree of order can also be controlled by the synthesis conditions. As all the compounds compared above were synthesized under conditions to maximize order, it should be adequate to compare them.

3.3. Electron Diffraction and Transmission Electron Microscopy. To gain further structural details and to check for the possibility of superstructures due to octahedral tilt twinning and/or compositional modulation, HRTEM and SAED studies were conducted. The data confirm the absence of any large superstructure but do provide additional information on the nature of the octahedral tilt system as well as reveal domain formation.

Figure 3 shows the selected area electron diffraction (SAED) pattern and high resolution transmission electron microscopy (HRTEM) image of a crystal of $NaLaInNbO_6$ along the $[\bar{1}10]_p$ zone axis. The pattern has been indexed and the image interpreted on the basis of the cubic a_p parameter with the aim of relating the extra reflections to the different structural aspects resulting in the superlattice. In addition to the Bragg reflections of the perovskite, there are superlattice reflections at $G_p \pm 1/2(111)^*$ (indicated with red arrow), which are associated with rock-salt-type ordering of the In and Nb atoms. In addition, reflections at $G_p \pm 1/2(001)^*$ (indicated with yellow arrow) are ascribed to layered-type ordering of the Na and La atoms. The contrast differences in the HRTEM image show periodicity in agreement with the extra reflections mentioned. Strong contrast differences giving a $\sqrt{2}a_p$ periodicity are characteristic of rock-salt-type ordering of cations,[55] since $\sqrt{2}a_p$ periodicity associated with tilting of the octahedra anion-sublattice is the origin of very weak contrast differences. The $2a_p$ periodicity along the $[001]_p$ direction is due to the layered-type ordering of the Na and La atoms. The FFT of the image, which is similar to the SAED pattern, is also shown in the inset of Figure 3b.

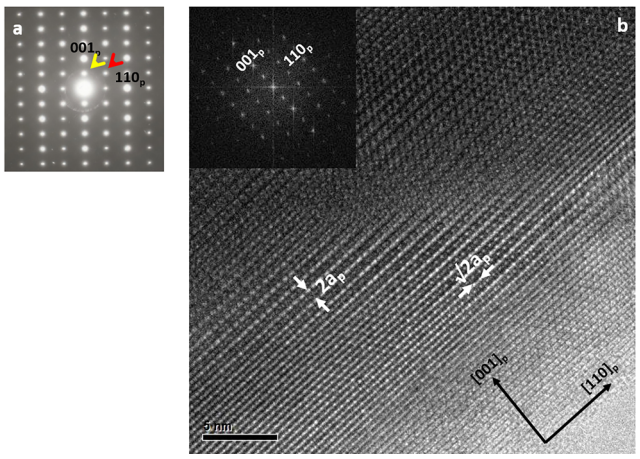

Figure 3. SAED pattern (a) and HRTEM image (b) along the $[\bar{1}10]_p$ zone axis of a crystal of $NaLaInNbO_6$. FFT of the image is included for comparison to the SAED pattern.

Figure 4 depicts the SAED pattern along, apparently, the $[010]_p$ zone axis, and the HRTEM images of three different areas of a crystal of $NaLaInNbO_6$ (the FFTs of the images are also included). The pattern and FFTs are also indexed according to the cubic perovskite like in Figure 3. The SAED pattern shows extra reflections at both $G_p \pm 1/2(001)^*$ and $G_p \pm 1/2(100)^*$, indicated by yellow arrows, which might be related to $2a_p$ periodicity along two perpendicular directions of the crystal structure. However, the image in Figure 4b clearly shows contrast differences in agreement with $2a_p$ periodicity along two perpendicular directions but which correspond to two different domains, and its FFT is similar to the SAED pattern. On the contrary, the image in Figure 4c corresponds to one domain along the $[010]_p$ zone axis and shows contrast differences corresponding to $2a_p$ periodicity only along one direction, and in agreement with the image, the corresponding FFT shows only extra reflections at $G_p \pm 1/2(001)^*$. The image in Figure 4d shows three different domains perpendicularly oriented, since $2a_p$ periodicity is observed along two perpendicular directions (within two different domains) and there is also one domain (surrounded by yellow) with contrast differences characteristic of the perovskite. Therefore, the

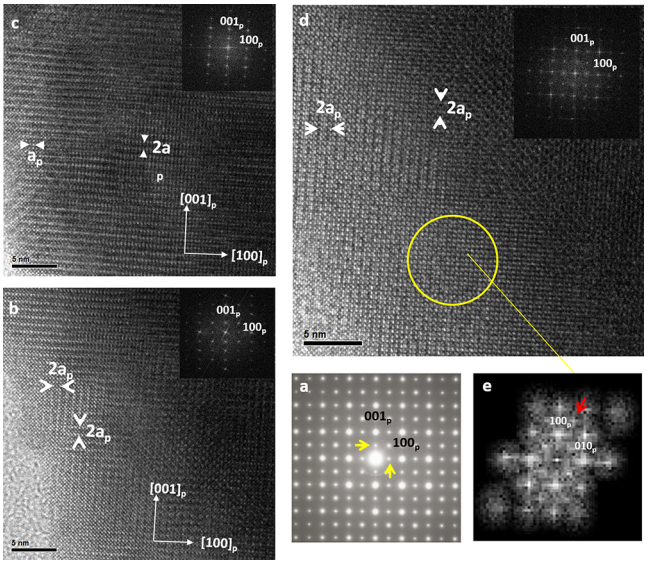

Figure 4. SAED pattern (a) and HRTEM images of different regions (b–d) along the $[010]_p$ zone axis of a crystal of $NaLaInNbO_6$. FFTs of the images are included.

DOI: 10.1021/acs.inorgchem.9b02050
Inorg. Chem. 2019, 58, 14058–14067

combination of the images and FFTs of the different areas of the crystal reveals that it is formed by three different domains with perpendicular orientation of the $\sqrt{2}a_p \times \sqrt{2}a_p \times 2a_p$ unit cell. Figure 4e shows the FFT of this last domain, which corresponds to the $[001]_p$ zone axis. The $1/2(110)_p$ reflection, also observed in the pattern in Figure 3a, probably appears due to multiple diffractions. Reflections are also observed at 1/2(ooe) with $h \neq k$ (o means odd and e means even) as indicated by a red arrow. These reflections can also be seen in the SAED pattern of Figure 4a, since this pattern is formed by the combination of the three patterns corresponding to each of the three different domains. The reflections at 1/2(ooe) with $h \neq k$ are ascribed to in-phase tilting of the octahedral network along the *c*-axis.[56] The rock-salt-type ordering of the In and Nb atoms and the domain formation prevent the assessment of the possible existence of in-phase or out-of-phase tilting along the other two main axes. However, if long-range in-phase tilting was present about these axes, this would lead to monoclinic $P2_1$ symmetry and clear peak splitting in the XRD pattern. As such splitting is not observed, the ED data suggest that $a^0a^0c^+$ tilting may be present within each domain. However, the low resolution of the FFT in Figure 4e (due to the small size of the domain) does not allow us to draw a firm conclusion. The SAED patterns and HRTEM images of $NaLaInTaO_6$ are similar to those of the Nb compound and are provided in the Supporting Information.

The observation of small domains in perovskites with partial cation ordering is reminiscent of many relaxor ferroelectrics.[57−60] While neither the $P4/nmm$ nor $P42_12$ space groups are polar, short-range tilting could create small regions with $P2_1$-like polar structures. Therefore, doubly ordered perovskites with small ordering domains such as these could represent an alternative to the conventional Pb and Bi based relaxor materials. Dielectric studies are suggested as a future research direction.

3.4. Prospects for Finding New $AA'BB'O_6$ Compounds. At the current point in the development of this field, it is worth considering how many of the possible members of this family of compounds have been discovered and what the likely compositions of the undiscovered members are. Perhaps the best way to classify these compositions is by their BB' combinations. Among the known members with +2/+6 oxidation states there are six groups of compounds, with members within a group differing by their *A*-site compositions (Table 1). The MgW, MnW, and CoW compounds comprise most known members of this family. For this group most of the lanthanides have been used with Na^+ already. The smaller lanthanides are generally not stable as they cause the tolerance factors to be too small, although high pressure synthesis has been used to make such phases.[45] K^+ has been used on the *A*-site as well for a MgW and a MnW member with La^{3+}. It might be possible to use a few other larger lanthanides with K^+, although the number is probably limited as there is evidence of destabilization as the size mismatch between the two *A*-site cations gets too large.[17,61] On the other hand, a KLu compound has been reported by a sol−gel method, so it might be possible to expand the number of K^+ compounds significantly.[33] Li^+ has also been used once, but other reports have identified issues with the stability of such compounds.[29,46] So, it is likely possible to obtain a few new members of the MgW, MnW, and CoW groups, but probably not a large number. The more promising place to look for new members is in the NiW, FeW, and CaW groups. These groups are much less explored and can likely be expanded into a larger series. Apart from finding new compositions, there is still work to be done resolving the structures of a number of the known compounds. Table 1 shows that there are several compounds that will likely show additional structural complexity if they are more carefully characterized.

Finding new +2/+6 groups might also be possible. Replacing W^{6+} with another SOJT such as Mo^{6+} has been attempted.[27,61] It does not seem that pure Mo^{6+} compounds are stable in the $AA'BB'O_6$ perovskite structure, although partial substitution of Mo^{6+} has been achieved.[27] Cr^{6+} is even less likely to be stable, so replacement of W^{6+} is probably not a promising path. Finding other +2 cations is the other possibility. Attempts have been made to use all of the first row transition metals with easily accessible +2 oxidation states. A trend has emerged that the stability tends to decrease as the electronegativity of the +2 cation increases.[17] Compounds with Mg^{2+}, Ca^{2+}, or Mn^{2+} form readily using basic ceramic synthesis, while most reports of compounds containing Fe^{2+}, Co^{2+}, or Ni^{2+} used wet or high pressure methods to acquire the desired product.[13,17,18,22,45] Attempts to create Cu^{2+} and Zn^{2+} compounds have been reported, but none of them were successful.[17,61] High pressure routes might be able to make such compounds, but this remains to be seen. So far there are no reports of $AA'BB'O_6$ perovskites containing second or third row transition metals with a +2 oxidation state, since this oxidation state is not as common for these elements. There are few other possibilities such as Cd^{2+}, so there may be a few new +2/W^{6+} groups to discover.

Another route to finding new compounds is by looking at +3/+5 BB' combinations. This area is much less explored and has the added advantage that these compounds may have different structural and physical properties compared to the +2/+6 compounds. As demonstrated in this work, both Nb^{5+} and Ta^{5+} can serve as SOJT cations in this structure type. While there are a large number of possible +3 cations to choose from, the challenge is finding combinations where the *B*-site cation is large enough to promote order with the SOJT cation. Some compositions are already known but have disordered cations due to small size differences.[15] The InNb and InTa combinations can likely form the basis for two new series of compounds by substitution with smaller lanthanides or by replacement of Na^+ with K^+. The Sc^{3+} cation is also nearly as large as In^{3+} and has been demonstrated to order with Nb^{5+}.[14] It is likely that other ScNb compounds can be made with different *A*-site cations. No ScTa compounds have yet to be reported, although one attempt was reported.[61] The large Y^{3+} might be made to incorporate onto the *B*-site if sufficiently large *A*-site cations are used. A_2YNbO_6 and A_2YTaO_6 compounds are already known with high levels of *B*-site order.[62,63] It might be possible to get some second or third row transition metals to order with Nb^{5+} or Ta^{5+}, such as Ru^{3+} or Ir^{3+}, although the size difference is marginal. Replacement of In^{3+} with Ga^{3+} or Al^{3+} could also be attempted. Although the size difference is smaller in these cases, there are some ordered double perovskites known.[64] Using Al^{3+} has been unsuccessfully attempted before, but there are no reports of trying to use Ga^{3+}.[61] It should be noted that two new bismuth based ScNb compounds have been reported recently which seem to have the criteria for *A*-site ordering (*B*-site order and a SOJT cation) but do not display any.[53] It seems that perhaps the lone pair nature of Bi^{3+} may make it unsuitable for this structure

DOI: 10.1021/acs.inorgchem.9b02050
Inorg. Chem. 2019, 58, 14058−14067

type.[46] It is also likely that others researchers will imagine new possibilities that are not included here.

4. CONCLUSIONS

This study reports the preparation of two new doubly cation ordered perovskites and represents the first in-depth structural characterization of $AA'BB'O_6$ perovskites with +3/+5 B/B' combinations. $NaLaInNbO_6$ and $NaLaInTaO_6$ are the first $AA'BB'O_6$ perovskites to incorporate a main group element. Like most other members of this family, they are also the first reported compounds to contain their respective combinations of elements and therefore represent the first members of their quintinary phase diagrams. They possess a structural complexity which spans several length scales and have features not observed in any of the previously known members of this family. Nearly complete long-range ordering of the *B*-site cations is present, while the *A*-site cations show a lower degree of order which is fragmented into perpendicular domains. The octahedral tilt system is not well-determined but may consist of $a^0a^0c^+$ tilting within each domain and additional tilting about the other axes over even shorter length scales. The propensity of the *B*′-cation to undergo a second order Jahn−Teller distortion is found to be one factor that determines the degree of *A*-site cation ordering, the other being the degree of *B*-site ordering. The nanoscale structural complexity could lead to desirable dielectric properties in this type of compound. We hope this work encourages the discovery of additional $AA'BB'O_6$ compounds, particularly those with +3/+5 BB' combinations.

■ ASSOCIATED CONTENT

Supporting Information

The Supporting Information is available free of charge on the ACS Publications website at DOI: 10.1021/acs.inorgchem.9b02050.

Tables with results of the Rietveld refinements and SAED/HRTEM images of $NaLaInTaO_6$ (PDF)

■ AUTHOR INFORMATION

Corresponding Author

*E-mail: graham.king@lightsource.ca.

ORCID

Graham King: 0000-0003-1886-7254

Susana Garcia-Martin: 0000-0003-0729-4892

Notes

The authors declare no competing financial interest.

■ ACKNOWLEDGMENTS

G.K. is very grateful to Andrew Grosvenor and the University of Saskatchewan for allowing him access to the equipment used to perform the synthesis and providing the starting materials used. He would also like to thank Jeremiah Beam for assistance in using this equipment. The Saskatchewan Structural Sciences Centre (SSSC) is acknowledged for providing facilities to conduct this research. Funding from Canada Foundation for Innovation, Natural Sciences and Engineering Research Council of Canada and the University of Saskatchewan supports research at the SSSC. G.K. also thanks Joel Reid for assistance in collecting the synchrotron diffraction data. Research described in this paper was performed at the Canadian Light Source, which is supported by the Canada Foundation for Innovation, Natural Sciences and Engineering Research Council of Canada, the University of Saskatchewan, the Government of Saskatchewan, Western Economic Diversification Canada, the National Research Council Canada, and the Canadian Institutes of Health Research. S.G.-M. thanks MINECO for financial support with Project MAT2016-78362-C4-4-R and the ICTS Centro Nacional de Microscopía Electrónica of U.C.M. for technical assistance.

■ REFERENCES

(1) Howard, C. J.; Stokes, H. T. Group-Theoretical Analysis of Octahedral Tilting in Perovskites. *Acta Crystallogr., Sect. B: Struct. Sci.* **1998**, *B54*, 782−789.

(2) Stokes, H. T.; Kisi, E. H.; Hatch, D. M.; Howard, C. J. Group theoretical analysis of octahedral tilting in ferroelectric perovskites. *Acta Crystallogr., Sect. B: Struct. Sci.* **2002**, *B58*, 934−938.

(3) Lufaso, M. W.; Woodward, P. M. Jahn-Teller distortions, cation ordering and octahedral tilting in perovskites. *Acta Crystallogr., Sect. B: Struct. Sci.* **2004**, *B60*, 10−20.

(4) King, G.; Woodward, P. M. Cation ordering in perovskites. *J. Mater. Chem.* **2010**, *20*, 5785−5796.

(5) Lufaso, M. W.; Barnes, P. W.; Woodward, P. M. Structure prediction of ordered and disordered multiple octahedral cation perovskites using SPuDS. *Acta Crystallogr., Sect. B: Struct. Sci.* **2006**, *B62*, 397−410.

(6) Shimakawa, Y. A-site-ordered perovskites with intriguing physical properties. *Inorg. Chem.* **2008**, *47*, 8562−8570.

(7) Woodward, P. M.; Suard, E.; Karen, P. Structural Tuning of Charge, Orbital, and Spin Ordering in Double-Cell Perovskites Series between $NdBaFe_2O_5$ and $HoBaFe_2O_5$. *J. Am. Chem. Soc.* **2003**, *125*, 8889−8899.

(8) Avila-Brande, D.; King, G.; Urones-Garrote, E.; Subakti; Llobet, A.; Garcia-Martin, S. Structural Determination and Imaging of Charge Ordering and Oxygen Vacancies of the Multifunctional Oxides $REBaMn_2O_{6-x}$ (RE = Gd, Tb). *Adv. Funct. Mater.* **2014**, *24*, 2510−2517.

(9) Garcia-Martin, S.; Alario-Franco, M.; Ehrenberg, H.; Rodriguez-Carvajal, J.; Amador, U. Crystal Structure and Microstructure of Some $La_{2/3-x}Li_{3x}TiO_3$ Oxides: An Example of the Complementary Use of Electron Diffraction and Microscopy and Synchrotron X-ray Diffraction to Study Complex Materials. *J. Am. Chem. Soc.* **2004**, *126*, 3587−3596.

(10) Sekiya, T.; Yamamoto, T.; Torii, Y. Cation Ordering in $(NaLa)(MgW)O_6$ with the Perovskite Structure. *Bull. Chem. Soc. Jpn.* **1984**, *57*, 1859.

(11) Lopez, M. L.; Veiga, M. L.; Pico, C. Cation Ordering in distorted perovskites $(MLa)(MgTe)O_6$, M = Na, K. *J. Mater. Chem.* **1994**, *4*, 547−550.

(12) Arillo, M. A.; Gomez, J.; Lopez, M. L.; Pico, C.; Veiga, M. L. Structural and electrical characterization of new materials with perovskite structure. *Solid State Ionics* **1997**, *95*, 241−248.

(13) Arillo, A. M.; Gomez, J.; Lopez, M. L.; Pico, C.; Veiga, M. L. Structural characterization and properties of the perovskite $(NaLa)(MW)O_6$ (M = Co, Ni): two new members in the group-subgroup relations for the perovskite-type structures. *J. Mater. Chem.* **1997**, *7*, 801−806.

(14) Knapp, M. C.; Woodward, P. M. *A*-site cation ordering in $AA'BB'O_6$ perovskites. *J. Solid State Chem.* **2006**, *179*, 1076.

(15) Dachraoui, W.; Yang, T.; Liu, C.; King, G.; Hadermann, J.; Van Tendeloo, G.; Llobet, A.; Greenblatt, M. Short-Range Layered A-Site Ordering in Double Perovskites $NaLaBB'O_6$ (B = Mn, Fe; B′ = Nb, Ta). *Chem. Mater.* **2011**, *23*, 2398−2406.

(16) Young, J.; Stroppa, A.; Picozzi, S.; Rondinelli, J. M. Tuning the ferroelectric polarization in $AA'MnWO_6$ double perovskites through A cation substitution. *Dalton Trans.* **2015**, *44*, 10644.

(17) King, G.; Thimmaiah, S.; Dwivedi, A.; Woodward, P. M. Synthesis and Characterization of New $AA'BB'O_6$ Perovskites

DOI: 10.1021/acs.inorgchem.9b02050
Inorg. Chem. 2019, 58, 14058−14067

Exhibiting Simultaneous Ordering of *A*-site and *B*-site Cations. *Chem. Mater.* **2007**, *19*, 6451−6458.
(18) King, G.; Wayman, L. M.; Woodward, P. M. Magnetic and structural properties of Na*Ln*MnWO$_6$ and Na*Ln*MgWO$_6$ perovskites. *J. Solid State Chem.* **2009**, *182*, 1319−1325.
(19) Zuo, P.; Klein, H.; Darie, C.; Colin, C. V. Magnetic properties of the doubly ordered perovskite NaLnCoWO$_6$ (Ln = Y, La, Pr, Nd, Sm, Eu, Gd, Tb, Dy, Ho, Er, Yb) family. *J. Magn. Magn. Mater.* **2018**, *458*, 48−51.
(20) King, G.; Wills, A. S.; Woodward, P. M. Magnetic structures of Na*L*MnWO$_6$ perovskites (*L*=La, Nd, Tb). *Phys. Rev. B: Condens. Matter Mater. Phys.* **2009**, *79*, 224428.
(21) Fukushima, T.; Stroppa, A.; Picozzi, S.; Perez-Mato, J. M. Large ferroelectric polarization in the new double perovskite NaLaMnWO$_6$ induced by non-polar instabilities. *Phys. Chem. Chem. Phys.* **2011**, *13*, 12186−12190.
(22) Retuerto, M.; Li, M. R.; Ignatov, A.; Croft, M.; Ramanujachary, K. V.; Chi, S.; Hodges, J. P.; Dachraoui, W.; Hadermann, J.; Tran, T. T.; Halasyamani, P. S.; Grams, C. P.; Hemberger, J.; Greenblatt, M. Polar and Magnetic Layered A-site and Rock Salt B-Site Ordered NaLnFeWO$_6$ (Ln = La, Nd) Perovskites. *Inorg. Chem.* **2103**, *52*, 12482−12491.
(23) Blasco, J.; Rodríguez-Velamazán, J. A.; Subías, G.; García-Muñoz, J. L.; Stankiewicz, J.; García, J. Spin Ordering and Physical Properties of NaPrFeWO$_6$ and NaSmFeWO$_6$ with Polar Double Perovskite Structure. *Acta Mater.* **2019**, A-19-527.
(24) De, C.; Kim, T. H.; Kim, K. H.; Sundaresan, A. The absence of ferroelectric polarization in layered and rock-salt ordered NaLnMnWO$_6$ (Ln = La, Nd, Tb) perovskites. *Phys. Chem. Chem. Phys.* **2014**, *16*, 5407.
(25) De, C.; Sundaresan, A. Nonswitchable polarization and magnetoelectric coupling in the high-pressure synthesized doubly ordered perovskites NaYMnWO$_6$ and NaHoCoWO$_6$. *Phys. Rev. B: Condens. Matter Mater. Phys.* **2018**, *97*, 214418.
(26) Hou, J.; Yin, X.; Huang, F.; Jiang, W. Synthesis and photoluminescence properties of NaLaMgWO$_6$:RE^{3+} (RE = Eu, Sm, Tb) phosphor for white LED applications. *Mater. Res. Bull.* **2012**, *47*, 1295−1300.
(27) Zhang, L.; Lu, Z.; Han, P.; Wang, L.; Zhang, Q. Synthesis and photoluminescence of Eu^{3+} activated double perovskite NaGdMg(W,Mo)O$_6$ − a potential red phosphor for solid state lighting. *J. Mater. Chem. C* **2013**, *1*, 54.
(28) Sharits, A. R.; Khoury, J. F.; Woodward, P. M. Evaluating NaREMgWO$_6$ (RE = La, Gd, Y) Doubly Ordered Double Perovskites as Eu^{3+} Phosphor Hosts. *Inorg. Chem.* **2016**, *55*, 12383−12390.
(29) Zhang, Z.-W.; Qi, H.-X.; Zhu, X.-Y.; Lv, R.-J.; Hou, J.-W.; Li, J.; Wang, D.-J. Photoluminescence of a Novel Red Emitting Phosphor LiLaMgWO$_6$. *Russian Jouranl of Physcial Chemistry A* **2017**, *91*, 785−790.
(30) Liang, Y.; Noh, H. M.; Ran, W.; Park, S. H.; Choi, B. C.; Jeong, J. H.; Kim, K. H. The design and synthesis of new double perovskite (Na,Li)YMg(W,Mo)O$_6$:Eu^{3+} red phosphors for white light emitting diodes. *J. Alloys Compd.* **2017**, *716*, 56−64.
(31) Ran, W.; Noh, H. M.; Moon, B. K.; Park, S. H.; Jeong, J. H.; Kim, J. H.; Liu, G.; Shi, J. Crystal structure, electronic structure and photoluminescence properties of KLaMgWO$_6$:Eu^{3+} phosphors. *J. Lumin.* **2018**, *197*, 270−276.
(32) Yang, Q.; Li, G.; Wei, Y.; Chai, H. Synthesis and photoluminescence properties of red-emitting NaLaMgWO$_6$:Sm^{3+},Eu^{3+} phosphors for white LED applications. *J. Lumin.* **2018**, *199*, 323−330.
(33) Li, Q.; Zhang, L.; Zhen, F.; Wei, S.; Bu, W.; Yao, Q.; Jiang, Z.; Chen, H. Photoluminescence enhancement of novel K(Y,Lu)CaWO$_6$:Eu^{3+} red phosphor prepared by controllable citrate-EDTA complexing method. *Ceram. Int.* **2018**, *44*, 15565−15571.
(34) Ran, W.; Noh, H. M.; Park, S. H.; Lee, B. R.; Kim, J. H.; Jeong, J. H.; Shi, J. Er^{3+}-Activated NaLaMgWO$_6$ double perovskite phosphors and their bifunctional application in solid-state lighting and non-contact optical thermometry. *Dalton Trans.* **2019**, *48*, 4405.
(35) Kumar, K. N.; Vijayalakshmi, L.; Choi, J. Investigation of Upconversion Photoluminescence of Yb^{3+}/Er^{3+}:NaLaMgWO$_6$ Noncytotoxic Double Perovskite Nanophosphors. *Inorg. Chem.* **2019**, *58*, 2001−2011.
(36) King, G.; Garcia-Martin, S.; Woodward, P. M. Octahedral tilt twinning and compositional modulation in NaLaMgWO$_6$. *Acta Crystallogr., Sect. B: Struct. Sci.* **2009**, *B65*, 676−683.
(37) Abakumov, A. M.; Erni, R.; Tsirlin, A. A.; Rossell, M. D.; Batuk, D.; Nenert, G.; Van Tendeloo, G. Frustrated Octahedral Tilting Distortion in the Incommensurately Modulated Li$_{3x}$Nd$_{2/3-x}$TiO$_3$ Perovskites. *Chem. Mater.* **2013**, *25*, 2670−2683.
(38) Garcia-Martin, S.; Urones-Garrote, E.; Knapp, M. C.; King, G.; Woodward, P. M. Transmission Electron Microscopy Studies of NaLaMgWO$_6$: Spontaneous Formation of Compositionally Modulated Stripes. *J. Am. Chem. Soc.* **2008**, *130*, 15028−15037.
(39) Garcia-Martin, S.; King, G.; Urones-Garrote, E.; Nenert, G.; Woodward, P. M. Spontaneous Superlattice Formation in the Doubly Ordered Perovskite KLaMnWO$_6$. *Chem. Mater.* **2011**, *23*, 163−170.
(40) Licurse, M. W.; Borisevich, A. Y.; Davies, P. K. Nanoscale modulations in (KLa)(CaW)O$_6$ and (NaLa)(CaW)O$_6$. *J. Solid State Chem.* **2012**, *191*, 220−224.
(41) Garcia-Martin, S.; Urones-Garrote, E.; King, G.; Woodward, P. M. Comment on Frustrated Octahedral Tilting Distortion in the Incommensurately Modulated Li$_{3x}$Nd$_{2/3-x}$TiO$_3$ Perovskites. *Chem. Mater.* **2014**, *26*, 1286−1287.
(42) Zuo, P.; Darie, C.; Colin, C. V.; Klein, H. Investigation of the Structure of the Modulated Doubly Ordered Perovskite NaLaCoWO$_6$ and Its Reversible Phase Transition with a Colossal Temperature Hysteresis. *Inorg. Chem.* **2019**, *58*, 81−92.
(43) Licurse, M. W.; Davies, P. K. Nanocheckerboard modulations in (NaNd)(MgW)O$_6$. *Appl. Phys. Lett.* **2010**, *97*, 123101.
(44) Garcia-Martin, S.; King, G.; Nenert, G.; Ritter, C.; Woodward, P. M. The Incommensurately Modulated Structures of the Perovskites NaCeMnWO$_6$ and NaPrMnWO$_6$. *Inorg. Chem.* **2012**, *51*, 4007−4014.
(45) Zuo, P.; Colin, C. V.; Klein, H.; Bordet, P.; Suard, E.; Elkaim, E.; Darie, C. Structural Study of a Doubly Ordered Perovskite Family NaLnCoWO$_6$ (Ln = Y, La, Pr, Nd, Sm, Eu, Gd, Tb, Dy, Ho, Er, Yb): Hybrid Improper Ferroelectricity in Nine New Members. *Inorg. Chem.* **2017**, *56*, 8478−8489.
(46) Knapp, M. C. *Dissertation*; Investigations into the structure and properties of ordered perovskites, layered perovskites, and defect pyrochlores. Ohio State University, 2006.
(47) Tarvin, R.; Davies, P. K. A-Site and B-Site Order in (Na$_{1/2}$La$_{1/2}$)(Mg$_{1/3}$Nb$_{2/3}$)O$_3$ Perovskite. *J. Am. Ceram. Soc.* **2004**, *87*, 859−863.
(48) Ting, V.; Liu, Y.; Withers, R. L.; Noren, L.; James, M.; Fitz Gerald, J. D. A structure and phase analysis investigation of the "1:1" ordered A_2InNbO$_6$ (A = Ca^{2+}, Sr^{2+}, Ba^{2+}). *J. Solid State Chem.* **2006**, *179*, 551−562.
(49) Zhou, Q.; Kennedy, B. J.; Avdeev, M. Crystal structures and phase transitions in Sr$_2$InTaO$_6$ perovskite. *Phys. Chem. Miner.* **2013**, *40*, 603−610.
(50) Zhou, Q.; Tan, T.-Y.; Kennedy, B. J.; Hester, J. R. Crystal structures and phase transitions in Sr doped Ba$_2$InTaO$_6$ perovskites. *J. Solid State Chem.* **2013**, *206*, 122−128.
(51) Toby, B. H.; Von Dreele, R. B. GSAS-II: the genesis of a modern open-source all purpose crystallography software package. *J. Appl. Crystallogr.* **2013**, *46*, 544−549.
(52) Dachraoui, W.; Hadermann, J.; Abakumov, A. M.; Tsirlin, A. A.; Batuk, D.; Glazyrin, K.; McCammon, C.; Dubrovinsky, L.; Van Tendeloo, G. Local Oxygen-Vacancy Ordering and Twinned Octahedral Tilting Pattern in the Bi$_{0.81}$Pb$_{0.91}$FeO$_{2.905}$ Cubic Perovskite. *Chem. Mater.* **2012**, *24*, 1378−1385.
(53) Surta, T. W.; Manjon-Sanz, A.; Qian, E.; Tran, T. T.; Dolgos, M. R. Low Temperature synthesis route and structural characterization of (Bi$_{0.5}$A$_{0.5}$)(Sc$_{0.5}$Nb$_{0.5}$)O$_3$ (A = K$^+$ and Na$^+$) perovskites. *Inorg. Chem. Front.* **2018**, *5*, 1033−1044.
(54) Ok, K. M.; Halasyamani, P. S.; Casanova, D.; Llunell, M.; Alemany, P.; Alvarez, S. Distortions in Octahedrally Coordinated d^0

DOI: 10.1021/acs.inorgchem.9b02050
Inorg. Chem. 2019, 58, 14058−14067

Transition Metal Oxides: A Continuous Symmetry Measures Approach. *Chem. Mater.* **2006**, *18*, 3176−3183.
(55) Senn, M. S.; Chen, W.; Saito, T.; Garcia-Martin, S.; Attfield, J. P.; Shimakawa, Y. B-Cation Order Control of Magnetism in the 1322 Perovskite $CaCu_3Fe_2Nb_2O_{12}$. *Chem. Mater.* **2014**, *26*, 4832−4837.
(56) Woodward, D. I.; Reaney, I. M. Electron diffraction of tilted perovskites. *Acta Crystallogr., Sect. B: Struct. Sci.* **2005**, *B61*, 387−399.
(57) Blinc, R.; Laguta, V.; Zalar, B. Field Cooled and Zero Field Cooled ^{207}Pb NMR and the Local Structure of Relaxor $PbMg_{1/3}Nb_{2/3}O_3$. *Phys. Phys. Rev. Lett.* **2003**, *91*, 247601.
(58) Jeong, I.-K.; Darling, T. W.; Lee, J. K.; Proffen, Th.; Heffner, R. H.; et al. Direct Observation of the Formation of Polar Nanoregions in $Pb(Mg_{1/3}Nb_{2/3})O_3$ Using Neutron Pair Distribution Function Analysis. *Phys. Rev. Lett.* **2005**, *94*, 147602.
(59) Bokov, A. A.; Ye, Z.-G. Recent progress in relaxor ferroelectric with perovskite structure. *J. Mater. Sci.* **2006**, *41*, 31−52.
(60) Peters, J. J. P.; Sanchez, A. M.; Walker, D.; Whatmore, R.; Beanland, R. Quantitative High-Dynamic-Range Electron Diffraction of Polar Nanodomains in Pb_2ScTaO_6. *Adv. Mater.* **2019**, *31*, 1806498.
(61) King, G. *Structural, Magnetic, and Electronic Studies of Complex Perovskites*. Dissertation, The Ohio State University, 2010.
(62) Zhou, Q.; Kennedy, B. J.; Avdeev, M. Structural studies of the disorder and phase transitions in the double perovskite Sr_2YTaO_6. *J. Solid State Chem.* **2010**, *183*, 1741−1746.
(63) Zhou, Q.; Kennedy, B. J.; Kimpton, J. A. The effect of disorder in Ba_2YTaO_6 on the tetragonal to cubic phase transition. *J. Solid State Chem.* **2011**, *184*, 729−734.
(64) Barnes, P. W.; Lufaso, M. W.; Woodward, P. M. Structure determination of $A_2M^{3+}TaO_6$ and $A_2M^{3+}NbO_6$ ordered perovskites: octahedral tilting and pseudosymmetry. *Acta Crystallogr., Sect. B: Struct. Sci.* **2006**, *B62*, 384−396.

DOI: 10.1021/acs.inorgchem.9b02050
Inorg. Chem. 2019, 58, 14058−14067